Available online at www.sciencedirect.com
SCIENCE DIRECT®
Journal of Solid State Chemistry 177 (2004) 721–724
JOURNAL OF SOLID STATE CHEMISTRY
http://elsevier.com/locate/jssc

Synthesis and morphology control of nanocrystalline boron nitride

Liang Shi,[a,b] Yunle Gu,[a] Luyang Chen,[a] Yitai Qian,[a,*] Zeheng Yang,[a] and Jianhua Ma[a]

[a] *Structure Research Laboratory and Department of Chemistry, University of Science and Technology of China, Hefei, Anhui 230026, China*
[b] *Department of Materials Science and Engineering, University of Science and Technology of China, Hefei 230026, China*

Received 26 June 2003; received in revised form 15 August 2003; accepted 20 August 2003

Abstract

Nanocrystalline boron nitride (BN) with needle-like and hollow spherical morphology has been synthesized by nitriding of MgB_2 with NH_4Cl and NH_4Cl–NaN_3, respectively. The amount of NaN_3 has an obvious effect on the size of the hollow spheres. The samples were characterized by X-ray powder diffraction, Fourier transformation infrared spectroscopy, X-ray photoelectron spectra, and transmission electron microscopy. The possible mechanism of morphology control is also discussed.

Keywords: Chemical synthesis; Hexagonal boron nitride; Morphology control; Characterization

1. Introduction

Boron nitride, BN, is well known for its unique physical and chemical properties, such as supreme hardness (for cubic BN), low density (for hexagonal BN), high temperature stability, high thermal conductivity, high melting point, low dielectric constant and chemical inertness. Due to these properties, boron nitride has been used widely in various areas. For example, boron nitride can be applied in cutting tools, grinding, refractory, lubricants, electrical insulators and so forth [1–3].

Various synthesis methods have been reported for preparation of boron nitride, such as the carbothermic reduction of boric oxide [4], the direct reaction of boron and nitrogen [5], pyrolysis of $(HBNH)_3$ [6], direct nitriding of boric acid with ammonia gas [7]. Recently, Hu et al. [8] reported that nanocrystalline BN with a whisker–like morphology could be synthesized by the reaction of KBH_4 and NH_4Cl at 650°C, Hao et al. [9] synthesized nanocrystalline cubic BN particles by reacting Li_3N and BBr_3 at low-temperature benzene thermal conditions, Yang et al. [10,11] synthesized nanocrystalline cubic BN by pulsed laser-induced liquid–solid interfacial reaction. In addition, other methods have been developed to prepare BN nanotubes, nanowires and nanocapsules [12–15].

Here we reported a chemical route to synthesize nanocrystalline hexagonal boron nitride (hBN) with needle-like or hollow spherical morphology. The reaction was carried out in an autoclave and can be described as follows:

$$2NH_4Cl + MgB_2 \rightarrow 2BN + MgCl_2 + 4H_2,$$
$$5NH_4Cl + 2MgB_2 + NaN_3 \rightarrow 4BN + 2MgCl_2 + 10H_2 + NaCl + 2N_2.$$

2. Experimental

In a typical procedure, an appropriate amount of NH_4Cl (0.05 mol) and MgB_2 (0.025 mol) were put into a stainless autoclave of 50 ml capacity (route 1); in another procedure, appropriate excess NaN_3 (molar ratio of NaN_3 to NH_4Cl to be 0.5:1 and 1:1, respectively) was also added into the autoclave (route 2). The autoclave was sealed and maintained at 550°C for 8 h in route 1 or maintained at 500°C for 8 h in route 2, then cooled to room temperature. The product was washed with absolute ethanol and distilled water to remove NaCl, $MgCl_2$ and other impurities. After drying in vacuum at 60°C for 4 h, the final white powder product was obtained.

*Corresponding author. Fax: +86-551-363-1760.
E-mail addresses: sliang@ustc.edu.cn (L. Shi), ytqian@ustc.edu.cn (Y. Qian).

0022-4596/$ - see front matter © 2003 Published by Elsevier Inc.
doi:10.1016/j.jssc.2003.08.026

X-ray powder diffraction (XRD) pattern was carried out on a Rigaku Dmax-γA X-ray diffractometer with Cu$K\alpha$ radiation ($\lambda = 1.54178$ Å). Fourier transformation infrared spectroscopy (FTIR) spectra were measured on a Shimadzu IR-400 spectrometer with the KBr pressed disks. The morphology of nanocrystalline hBN was observed from transmission electron microscopy (TEM) images taken with a Hitachi H-800 transmission electron microscope. X-ray photoelectron spectra (XPS) were recorded on a VGESCALAB MKII X-ray photoelectron spectrometer, using non-monochromatized Mg$K\alpha$ X-rays as the excitation source.

3. Results and discussion

Fig. 1 shows the XRD patterns of the as-prepared BN samples from route 1 and route 2, all the peaks can be indexed as hexagonal BN. After refinement, the lattice constants are obtained. For BN sample from route 1, $a = 2.500$ Å, $c = 6.681$ Å; for BN sample from route 2, $a = 2.510$ Å, $c = 6.685$ Å, which is very close to the reported value for hBN ($a = 2.510$ Å, $c = 6.690$ Å, JCPDS card, No. 851068). The broadening of the XRD peaks may originate from the small grain sizes of the BN samples, which is confirmed by the TEM results.

Fig. 2 shows the FTIR spectra of the BN samples at room temperature. Two strong peaks around 1379 and 813 cm^{-1} could be observed clearly for samples from routes 1 and 2, which is assigned to the B–N stretching vibrations and B–N–B bending vibrations, respectively [16,17]. A weak peak around 3403 cm^{-1} could be attributed to the moisture absorbed on the surface of the sample.

Fig. 3 gives the XPS spectra of the BN sample from route 1. The B1 s and N1 s core-level regions were examined. It is found that the binding energy of B1 s is at 190.60 eV and N1 s at 398.30 eV, which is consistent with the reported value for BN [18]. It is also found that a π plasmon peak at approximately 9 eV away from the B1 s and N1 s peaks, which is a characteristic for hBN [19]. The qualification of the peak intensities reveals that the atomic ratio of B to N is 1.01:1.0, which agrees well with the chemical stoichiometric relation between B and N. The XPS spectra of the BN sample from route 2

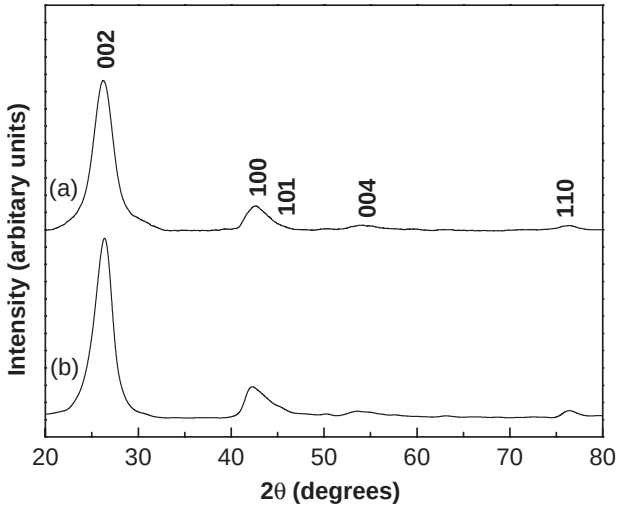

Fig. 1. XRD patterns of the BN sample: (a) route 1; (b) route 2.

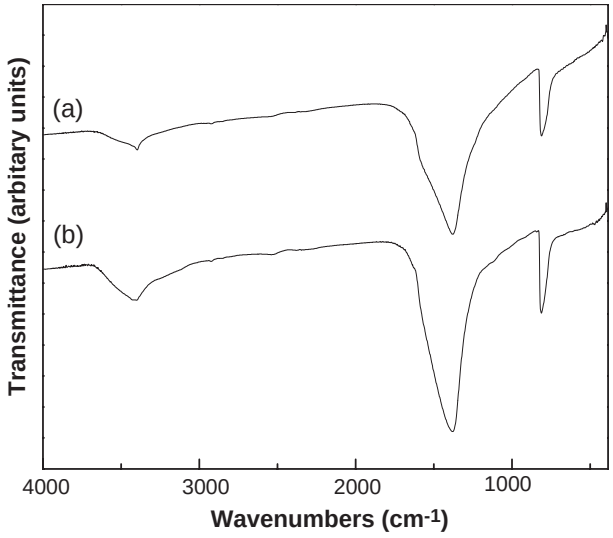

Fig. 2. FTIR spectra of the BN sample: (a) route 1; (b) route 2.

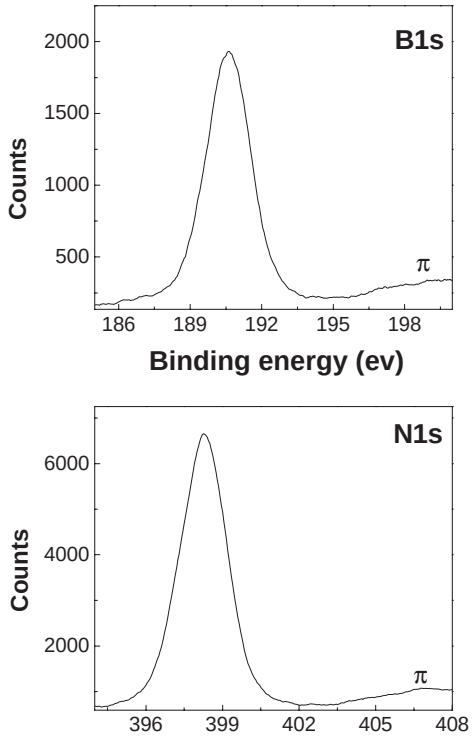

Fig. 3. XPS spectra of the BN sample from route 1.

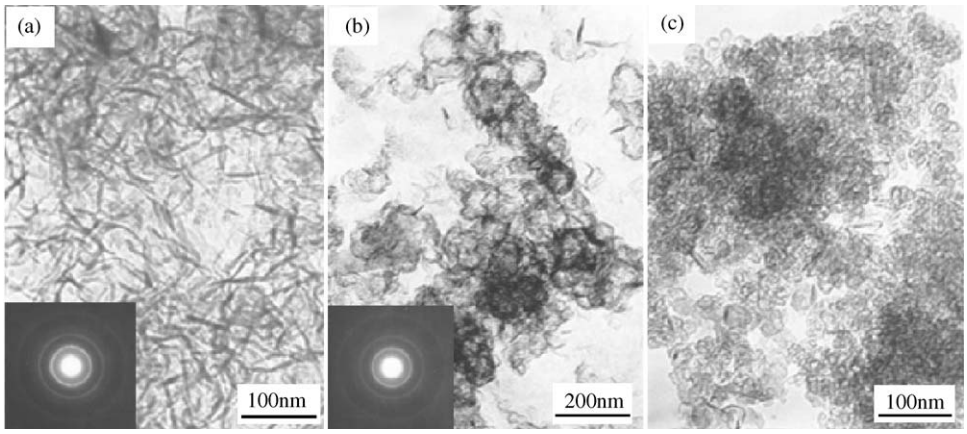

Fig. 4. TEM images and SAED patterns (inset) of the BN samples: (a) route 1; (b) route 2 with the molar ratio of NaN_3 to NH_4Cl of 0.5:1; (c) route 2 with the molar ratio of NaN_3 to NH_4Cl of 1:1.

(not shown) are similar to that of the BN sample from route 1.

The morphology of BN was investigated by TEM. Fig. 4a shows a typical TEM image of the BN sample from route 1. It reveals that the BN sample consists of uniform needle-like particles with an average size of $100 \times 8\,nm^2$. Fig. 4b shows a TEM image of the BN sample from route 2 with the molar ratio of NaN_3 to NH_4Cl of 0.5:1. It can be observed that the sample mainly consists of hollow spheres of 80–120 nm in diameters. Fig. 4c shows a TEM image of the BN sample from route 2 with the molar ratio of NaN_3 to NH_4Cl of 1:1. The sample still consists of hollow spheres, but average size is only about 20 nm. This suggests that the amount of NaN_3 may play an important role in the formation and size of BN hollow spheres. The insets of Fig. 4a and b show the selected area transmission electron diffraction (SAED) patterns of BN samples from routes 1 and 2 respectively. The diffraction rings from inner to outer, at d-spacings of 3.33, 2.16 and 1.25 Å for route 1, at *d*-spacings of 3.34, 2.17, 1.25 Å for route 2, match hBN (002), (100), (110) planes, in good agreement with the XRD results.

According to free energy calculations, synthetic routes 1 and 2 are thermodynamically spontaneously and highly exothermic (for route 1: $\Delta G = -65.05$ kcal/mol, $\Delta H = -50.2$ kcal/mol; for route 2: $\Delta G = -81.3$ kcal/mol, $\Delta H = -57.3$ kcal/mol). A great deal of heat was generated during the reaction process and resulted to an instantaneous local high temperature, which favors the formation of crystalline hBN. On the other hand, both synthesis routes could bring about high pressure in the autoclave due to the by-product, H_2 or/and N_2. High pressure in the autoclave is also beneficial to the formation of crystalline hBN. In comparison with the previous synthetic route in Ref. [8] reported by our group, no cubic BN was formed in present routes. This may be due to the absence of molten NaCl (melting point = 804°C) flux or $MgCl_2$ (melting point: = 714°C) as a result of lower reaction temperatures in present routes. The monovalent anion Cl^{-1} may play an important role in the formation of cBN because it could coordinate with B atoms on the hBN surface and cause it to undergo a structural change [8,20]. In route 2, NaN_3 decomposed generating N_2 and molten Na (melting point: 98°C) when the temperature increased up to 300°C. The molten metal Na acted as a solvent to mix the MgB_2 and NH_4Cl powders homogeneously. Meanwhile, the Na reacted with NH_4Cl and generated NH_3. The newly formed NH_3 bubbles dispersed in remained molten metal Na. At the desired temperature, MgB_2 would react with NH_3 on the surface of the bubbles and the hollow spherical BN was formed. In the case of reaction with the molar ratio of NaN_3 to NH_4Cl to be 0.5:1, a lot of NH_3 bubbles dispersed in a relatively small amount of remained unreacted Na obtained from NaN_3 decomposition. The small bubbles are readily to assembled into large bubbles. So the hollow sphere is relatively large. Whereas, when the molar ratio of NaN_3 to NH_4Cl is 1:1, the small NH_3 bubbles dispersed in a relatively large amount of molten Na. In addition, more N_2 was generated, which stirred the molten Na stronger. Due to these two factors, the NH_3 bubbles are hard to get together. Thus the hollow sphere is small.

The influence of the reaction temperature and time on the formation of BN was investigated. For route 1, it was found that little BN product could be obtained if the temperature is below 450°C. Heating at 500°C could produce BN, but the crystallinity was poor. An optimum temperature for nanocrystalline BN is about 550°C. As for route 2, BN cannot form at a temperature lower than 400°C. The reaction temperature we chose is 500°C. Varying the reaction time in the range of 4–10 h at 550°C for route 1 or at 500°C for route 2 did not

significantly affect the crystallinity. If the time is shorter than 3 h, the reaction becomes incomplete for both routes.

4. Conclusions

In summary, nanocrystalline hBN powders of the needle-like shape and nanometer-sized hollow spheres were successfully synthesized by nitriding of MgB_2 with NH_4Cl and NH_4Cl–NaN_3, respectively. The large amount of heat and high pressure generated during the reaction process favor the formation of crystalline BN. NaN_3 may play a key role in controlling the hollow spherical morphology of nanocrystalline hBN.

Acknowledgments

This work is supported by the National Natural Science Foundation of China and the 973 Projects of China.

References

[1] V. Laurence, D. Gerard, Etourneau, J. Mater. Sci. Eng. B 10 (1991) 149.
[2] S.S. Liouu, W.L. Worrel, Appl. Phys. A 49 (1989) 25.
[3] R.T. Paine, C.K. Narula, Chem. Rev. 90 (1990) 73.
[4] K.A. Schwetz, A. Lipp, in: W. Gerhartz et al. (Eds.), Ulmann's Encylopedia of Industrial Chemistry, Vol. 4, VCH, Weinheim, 1985, p. 295.
[5] J.B. Condon, C.E. Holcombe, D.H. Tohnson, L.M. Steckel, Inorg. Chem. 15 (1976) 2173.
[6] S. Hirano, T. Yogo, S. Asada, S. Naka, J. Am. Ceram. Soc. 72 (1989) 66.
[7] T. Kusunose, in: N.P. Bansal, K.V. Logan, J.P. Singh (Eds.), Innovative Processing and Synthesis: Ceramic, Glass and Composite, American Ceramic Society, Westerville, OH, 1997, pp. 443–454.
[8] Jun-Qing, Hu, Qing-Yi Lu, Kai-Bin Tang, 1, Shu-Hong Yu, Yi-Tai Qian, 1, Gui-En Zhou, Xian-Ming Liu, Jian-Xin Wu, J. Solid State Chem. 148 (1999) 325.
[9] X.P. Hao, D.L. Cui, G.X. Shi, Y.Q. Yin, X.G. Xu, J.Y. Wang, M.H. Jiang, X.W. Xu, Y.P. Li, B.Q. Sun, Chem. Mater. 13 (2001) 2457.
[10] J.B. Wang, G.W. Yang, C.Y. Zhang, X.L. Zhong, ZH.A. Ren, Chem. Phys. Lett. 367 (2003) 10.
[11] Q.X. Liu, G.W. Yang, J.X. Zhang, Chem. Phys. Lett. 373 (2003) 57.
[12] A. Loiseau, F. Willaime, N. Demoncy, G. Hug, H. Pascard, Phys. Rev. Lett. 76 (1996) 4737.
[13] D. Golberg, Y. Bando, M. Eremets, K. Takemura, K. Kurashima, H. Yusa, Appl. Phys. Lett. 69 (1996) 2045.
[14] N.G. Chopra, R.J. Luyken, K. Cherrey, V.H. Crespi, M.L. Cohen, S.G. Louie, A. Zettl, Science 269 (1995) 966.
[15] C.C. Tang, M. Lamy De La Chapella, P. Li, Y.M. Liu, H.Y. Dang, S.S. Fan, Chem. Phys. Lett. 342 (2001) 492.
[16] V. Cholet, L. Vandenbulcke, J.P. Rouan, P. Baillif, R. Erre, J. Mater. Sci. 29 (1994) 1417.
[17] S. Sadananda, K. Stefan, I. Lubica, M. Jana, B. Imre, S. Janos, J. Eur. Ceram. Soc. 18 (1998) 1037.
[18] C.D. Wagner, Handbook of X-ray Photoelectron Spectroscopy, Perkin-Elmer Corporation, Minnesota, 1979.
[19] D.H. Berms, M.A. Cappelli, J. Mater. Res. 12 (1997) 2014.
[20] Toshio Kobayshi Centeral Research Laboratory, Hitachi Ltd. Mater. Res. Bull. 14 (1979) 1541.